

# Solar Cruiser TRAC Boom Development

Lee Nguyen\*

Redwire Deployable Solutions, Longmont, CO, 80503

Zachary McConnel<sup>†</sup> and Kamron A. Medina<sup>‡</sup>

Redwire Deployable Solutions, Longmont, CO, 80503

Mark S. Lake<sup>§</sup>

Redwire Deployable Solutions, Longmont, CO, 80503

The TRAC boom studied is a 30 meter, high-aspect ratio and highly nonlinear structural element planned for the NASA Solar Cruiser spacecraft where it would serve as the solar sail's skeletal system designed to *deploy* the packaged reflective sail membrane as well as *support* operational sail tension loads for flight. Key design drivers for this boom are understanding and characterizing load-deformation behavior and quantifying buckling performance—under flight conditions (zero gravity). Knowing that the full-scale solar sail system cannot be feasibly tested for flight conditions under Earth's gravity, a building block approach is methodically followed to verify finite element analysis (FEA) predictions and to evolve the finite element model (FEM) accordingly, beginning with the lowest level complexity to match global elastic behavior to the highest level complexity to bound theoretical responses under conservative expected flight conditions. Although the testing campaign for the TRAC boom has not developed yet to produce a full-scale test data point that loads the boom to failure, the fidelity of simulations have evolved with success and warrant further interest and work on this high-aspect ratio, but highly stable, deployable *structural* boom.

## I. Nomenclature

$f$	=	flattened height
$h$	=	web height
$r$	=	flange radius
$t$	=	flange thickness
$t_o$	=	flange mid-plane offset from outer surface (nominally $t/2$ )
$\theta$	=	flare (subtended or included) angle
$y_c$	=	distance from web free edge to centroid
$x$	=	horizontal or in-plane direction
$y$	=	vertical or out-of-plane direction
$z$	=	boom axial direction

## II. Introduction

THE TRAC boom is a high strain composite (HSC) structure designed to sustain compressive and/or bending loads once deployed in space [1]. It is a thin shell open cross-section (Figure 1) structural element that can be flattened to allow for repeated elastic roll stowing and deployment. Compared with other spool-rolled booms, the TRAC boom cross-section provides the highest deployed second moment of inertia for a given flattened height resulting in a high torsional stiffness, which is largely the reason the design has gained recent acceptance for deploying large, lightweight structures in space [2, 3]. TRAC booms have been used to deploy solar sails for NASA's NanoSail-D mission, the

---

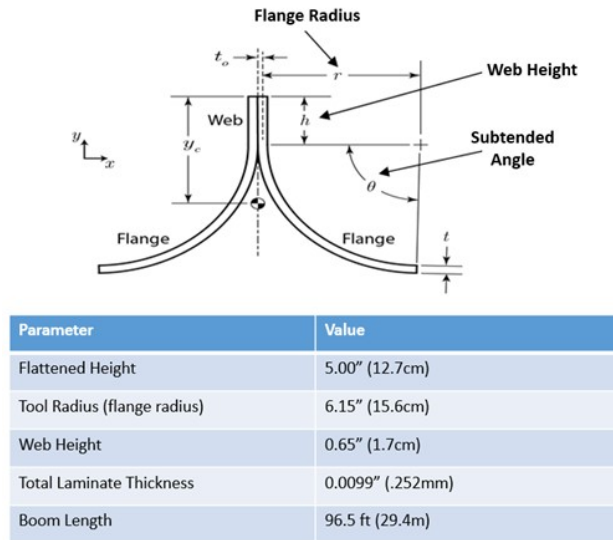
\*Sr. Structural Analysis Engineer IV, Redwire Deployable Solutions Longmont, 2602 Clover Basin Drive, Suite D.

<sup>†</sup>Sr. Prototyping Engineer III, Redwire Deployable Solutions Longmont, 2602 Clover Basin Drive, Suite D.

<sup>‡</sup>Sr. Mechanical Engineer, Redwire Deployable Solutions Longmont, 2602 Clover Basin Drive, Suite D.

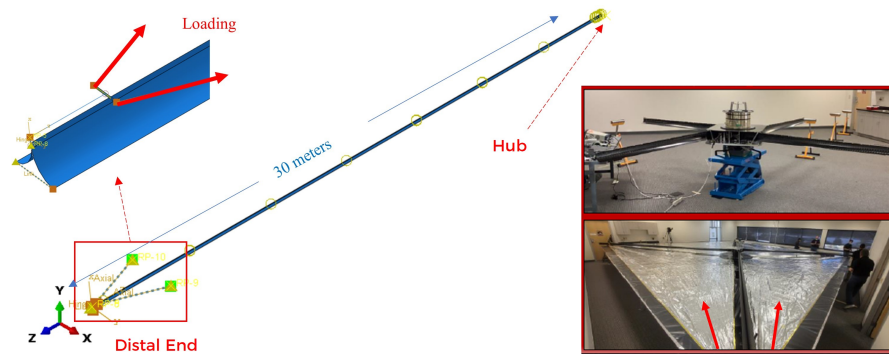
<sup>§</sup>Technical Fellow, Redwire Deployable Solutions Longmont, 2602 Clover Basin Drive, Suite D.

Planetary Society’s LightSail mission, and NASA’s upcoming NEA-Scout mission [4]. Redwire is currently developing 30m-long TRAC booms for NASA’s Solar Cruiser mission (Figure 2) [5].



**Fig. 1 TRAC Boom Geometry**

Despite the simplicity of its cross-section, the mechanics of TRAC boom structural behavior are complex and nonlinear, especially for slender TRAC booms under compression loading as is the case for the Solar Cruiser application. The challenge becomes finding an approach to characterize nonlinear behavior in order to verify that the design can satisfy key performance requirements, one of which is buckling strength. As shown in Figure 2, the global compression loading on the boom is similar to a classic Euler column loading condition. However, as illustrated in Table 1, the mechanical response and failure modes predicted for the TRAC boom can be very different using linear eigenvalue buckling analysis versus a nonlinear analysis approach. This paper discusses linear and nonlinear analysis methods applied to the development of the TRAC booms for the Solar Cruiser mission as well as accompanying critical sub-scale testing to support model-test correlation. Preliminary results of full-scale test articles will also be highlighted.



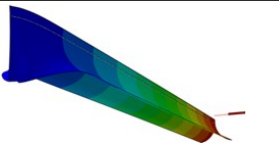

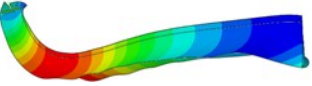

**Fig. 2 Solar Cruiser TRAC boom – General Loads and Boundary Conditions**

### III. TRAC Boom Architecture and Kinematic Control Features

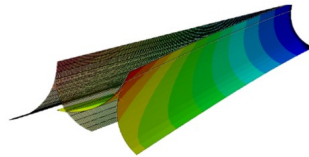
#### A. Basic Boom Architecture

The NASA Solar Cruiser application uses four TRAC booms that take on the basic geometries as shown in Figure 1. From legacy experience on the TRAC boom mechanics and basic normal modes assessment of this design, a key

**Table 1 Linear vs. Nonlinear Buckling Simulations**

	Displacements	Stress Contour
Eigenvalue Buckling Solution		
Implicit Dynamic Solution		

mode shape of interest or concern is the coupled lateral-torsional response as shown in Figure 3. This behavior is undesirable because, under load, the boom has the natural tendency to twist into a lower effective bending stiffness state—exacerbating global column buckling performance. Additionally, controlling tip positioning under load to minimize distal end displacements is not only desirable but also critical to the spacecraft’s momentum management control. These challenges guided the design features that will be outlined next.

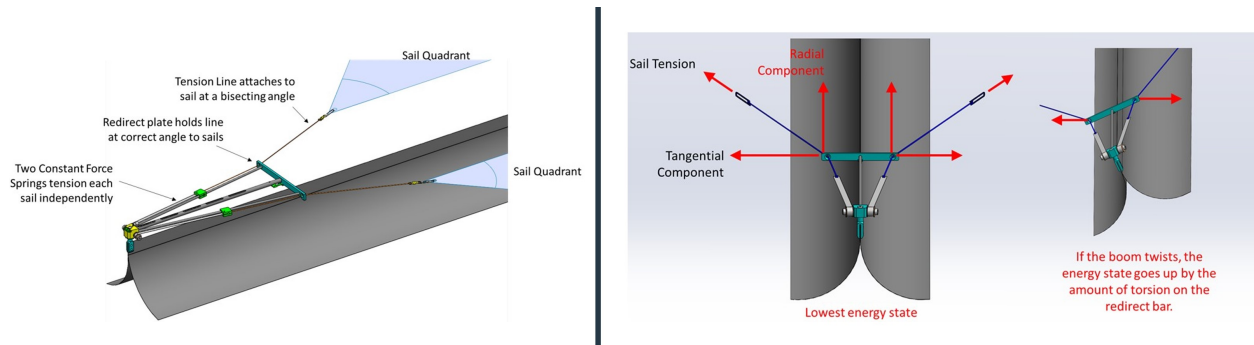


**Fig. 3 Lateral-Torsional Response Coupling**

**B. Kinematic Control Features**

*1. Distal End T-bar Assembly*

The first key kinematic management system in discussion is the distal end T-bar assembly\*. As showcased on the left of Figure 4, the distal end of each boom is joined to the corners of the two adjacent sail quadrants through the Distal Constant-Force Spring (CFS) assembly. This assembly allows for independent sail quadrant tensioning via constant force springs. The redirect plate changes the angle of the tensioning lines to match the direction of pull on the sail quadrants. The entire assembly is bonded to the web of the boom at its most distal point.

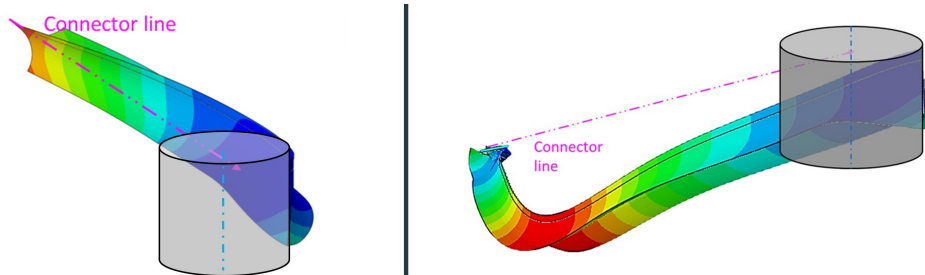


**Fig. 4 Distal End T-bar Assembly**

The distal end assembly, or “T-bar assembly”, inhibits lateral-torsional response coupling under compression loading. As the sail quadrants develop tension, they will begin to load the TRAC boom in compression. The lowest order buckling

\*Patent pending.

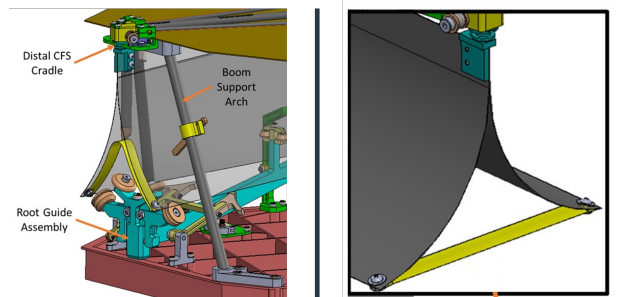
eigenmode of the boom is a lateral-torsional mode, as shown on the left of Figure 5. To practically stiffen the boom's response under continued loading, the T-bar assembly was conceived to control the buckling mode into a preferential direction. As the boom responds through lateral deflection and twist, the assembly rotates. This results in a net moment arm that the two sail quadrant tension lines must react across. As a result, the assembly 'corrects' its twist through positive feedback and restores its upright orientation. In this manner, the T-bar assembly is able to inhibit the lowest buckling eigenmode and shift the global instability to higher modes of buckling—as shown on the right of Figure 5.



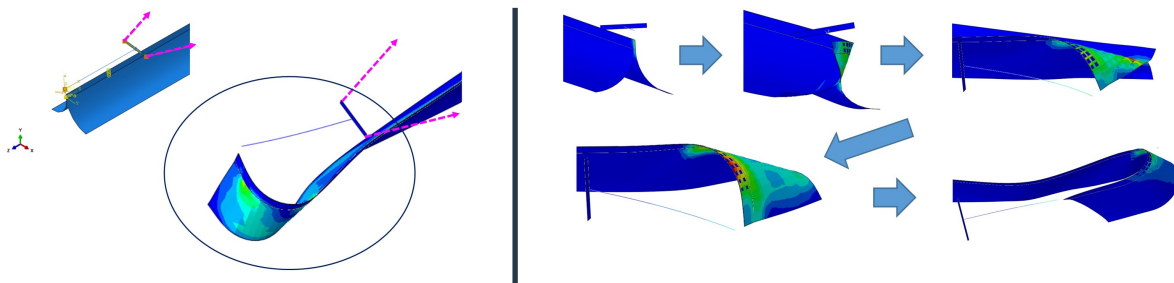
**Fig. 5 Load-Deformation Response without and with T-bar Assembly**

## 2. Distal Flange Tip Brace

With this improvement in buckling mode, the weakest link manifests at the distal end of the boom. Looking at Figure 6, additional treatments are then implemented with the distal flange tip brace<sup>†</sup>. A tape spring element connects the flange tips, and upon deployment, the cross-section recovers while the tape spring snaps into its straightened, load-carrying configuration.



**Fig. 6 Flange Tip Brace Stowed and Deployed**



**Fig. 7 Distal Collapse without Tip Brace**

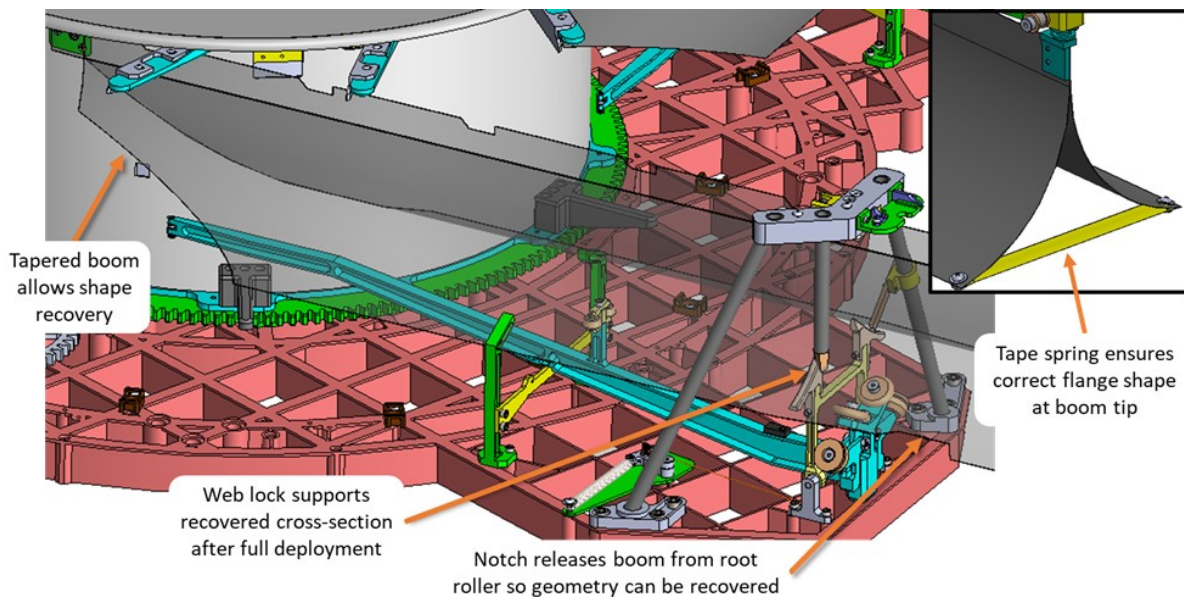
Through testing and analysis, it is demonstrated that without this feature, the failure mode arises from the flange halves closing onto each other followed by a rapid collapse of the boom as the cross-section flattens under load. Figure 7

<sup>†</sup>Patent pending.

illustrates this collapse simulation. With this kinematic constraint in place, we have shown the buckling performance improves further by inhibiting this distal end collapse.

### 3. Root Recovery Assembly

To improve the stability of the TRAC boom at the root end, the root recovery assembly<sup>‡</sup> mechanism was developed to enable the cross-section to completely recover upon full deployment—including a feature that braces the cross-section in its regained state. Figure 8 highlights several key features at the Sail Deployment Mechanism (SDM) that enable these kinematics. The web lock assembly is a mechanism that includes a wedge feature, referred to as the “web lock support”, that matches the regained flange radius and provides support ‘underneath’ the web to inhibit local instability. Not shown in Figure 8 are the mating wedges that interface against the boom support arch assembly. These wedges support ‘above’ the flanges and serve as the foundation against which the web lock support preloads. During deployment, the web lock support is spring tensioned against the bottom of the boom, and as the booms approach end of travel, the notch in the flanges releases them from the root guide assembly allowing enough space for the web lock to flip up and clamp the flanges into place. The boom flanges are tapered towards the spool tangency to dimensionally allow the cross-section to fully recover and not interfere with the spool surface itself. Axial compressive loads on the boom are reacted along the web region, where it is thicker than the flanges, and into a mounting tab to the spool. Additional supports can be seen in Figure 8 between the spool tangency and the arch support assembly that provide further support to the cross-section underneath the web as well as above the flanges. This mechanism is designed such that as the TRAC boom reaches the end of deployment, where it is designed to operate and develop nominal sail tension loads, the cross-section is constrained in its fully recovered configuration where buckling performance is optimized.



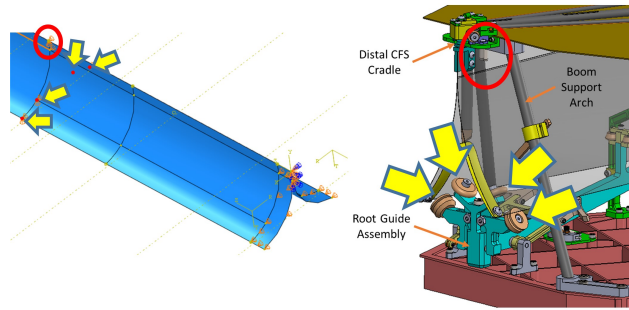
**Fig. 8 Root Recovery Features (with Tip Brace Deployed Inset)**

## IV. Finite Element Model and Assumptions

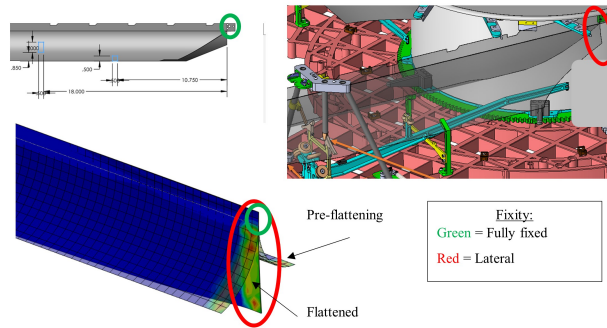
The finite element model (FEM) of the TRAC boom is built in Abaqus/CAE 2021. It contains 91,171 nodes. The element count is 82,306—of which 82,296 are linear quadrilateral reduced-integration elements of type S4R and 10 are linear line elements of type B31.

The FEM simulates the root boundary conditions reflective of the deploying configuration, including the flattened cross-section at the spool tangency point, as well as represents the distal flange tip brace and a T-bar assembly. Despite the nominal flight boundary conditions of the TRAC booms, as outlined in section III.B.3, the booms will be expected to provide load to the sail quadrants as they unspool the sail material from the hub during deployment. In this deploying

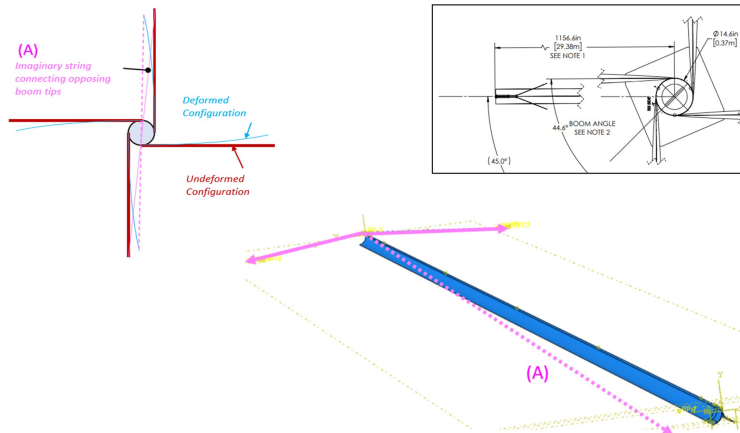
<sup>‡</sup>Patent pending.



**Fig. 9 FEM Boundary Conditions (1)**



**Fig. 10 FEM Boundary Conditions (2)**



**Fig. 11 TRAC Boom Loading Vector**

configuration, the root will not yet be recovered, so to conservatively bound the analysis, the FEM configuration will reflect root fixities, or end-conditions, as described below.

As shown in Figure 9, the boundary conditions at the root guide assembly are idealized with lateral and vertical constraints to simulate the support rollers at the root guide assembly, and lateral and vertical constraints to simulate the boom web location pin guide. Furthermore, as shown in Figure 10, once the root of the TRAC boom is flattened, a lateral constraint is imposed across the flange height while the web height is modeled with fully fixed constraints to idealize the spool mounting tab connection. Boom axial loads are reacted only in the web region of root. Note that the tapered profile of the flanges at the root-end is not accounted for in the FEM, as this added modeling complexity is

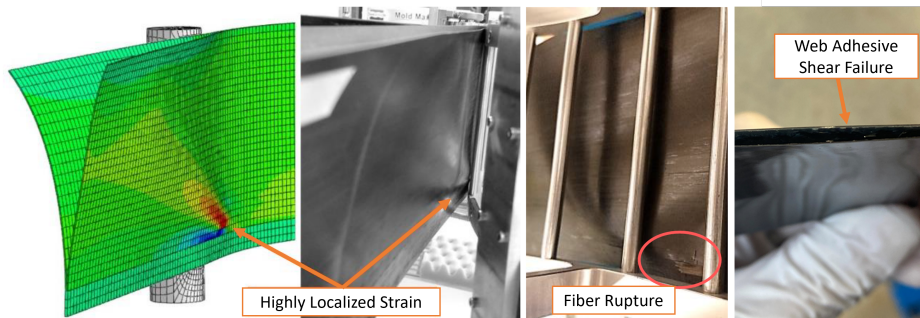
anticipated to not impact relevant responses or critical load paths of the global structure.

At the distal end, the T-bar assembly and flange tip brace are modeled, see Figure 7. The T-bar assembly is modeled using beam and shell elements and is represented in its locked configuration (does not swivel) using beam elements through the stand-off post in the FEM to reflect the fully-deployed operating condition. The flange tip brace is idealized as a link element; this feature is incorporated to prevent cross-sectional collapse and to optimize overall buckling behavior.

Loads due to sail tension are introduced via two axial connectors that follow vectors representative of fully deployed flight configuration. Per Figure 11, the assumption on global system-level deformation takes on the shape as a “pinwheel” response where each boom is expected to deform with its tip displacing towards the hub under load, and as such, the resultant loading vector for each TRAC boom is quantified with a line of action through the spool centerline axis.

## V. Material Properties, Geometry and Laminate Architecture

The laminate construction of the TRAC boom is optimized to balance the deployed stiffness and buckling strength requirements [6] of the boom along with considerations to ensure that the boom is both retractable and deployable. The boom geometry, laminate, and boom storage spool diameters are highly inter-related variables that impact the storage performance of a TRAC boom. The nature of these inter-related parameters requires an iterative design process to ensure that all of the deployed boom performance requirements are met while also ensuring that the boom can be packaged in the allotted storage volume. With regards to TRAC boom storage, there are three primary design constraints that must be considered: the minimum boom storage spool diameters to prevent inner-flange buckling during retraction, minimum boom storage spool diameters to prevent shear stress limitations of the adhesive and laminates inside of the bond region during retraction, and maximum boom storage spool diameters to prevent inner-flange buckling during deployment. Examples of boom failures with regards to some of these storage parameters are shown in Figure 12.



**Fig. 12 Inner Flange Buckling Fiber Rupture and Web Shear Failure**

Inner-flange buckling is a condition that can occur when the TRAC boom is wrapped around a spool. In this state, its inner flange is naturally under compression while the outer flange is in tension. A condition known as inner-flange buckling can occur when stowing or deploying where the inner flange will form a buckle. Upon stowing with a buckle condition, further spooling will cause the buckle to travel with the boom and past (underneath) compaction rollers, which increases stress locally along the bond line at the web. As the size of this buckle increases, the risk of rupturing the bond line increases. In addition to the inner-flange buckling constraints, shear stress in the bond region of the boom can lead to laminate and bond adhesive failures during retraction. Both of these phenomenon as well as the constraints that they place on boom geometry and minimum storage hub diameter have been previously published by Cox and Leclerc [4,6-8].

A secondary inner-flange buckling limitation occurs during the deployment of a TRAC boom. Similarly to slit-tube booms, TRAC booms have a natural localized buckling diameter that can be derived by minimizing the total strain energy of a TRAC boom cross section subject to bending about a hub [9]. This buckling diameter places an upper-bound limit on the maximum spool diameter of a TRAC boom during deployment. When a boom is stowed to a diameter close to or greater than this natural buckling diameter, the minimum energy state of the boom manifests as localized inner-flange buckles—especially in the outer wraps of the spool. The impact of this localized buckle is similar to that of an inner-flange buckle during retraction. As buckles form in the outer spool, without the presence of a positive tension load [9], they tend to get trapped behind compaction rollers on the spool. As deployment continues, the magnitude of

these localized buckles continues to grow typically leading to failure in the bond region to flange region interface of the boom.

The optimized laminate construction produces the resulting mechanical properties as shown in Tables 2, 3 and 4. In addition to the laminate mechanical properties, the overall thickness is  $2.52E-04$  m, and the overall density is  $1.55E + 06g/m^3$ . The geometry of the boom cross-section is defined in section III.A.

**Table 2 [A] Matrix (N/m)**

2.84E+07	4.09E+06	0.00E+00
4.09E+06	1.70E+07	6.98E-10
0.00E+00	6.98E-10	4.47E+06

**Table 3 [B] Matrix (N)**

-3.69E-13	8.88E-14	-3.55E-14
8.88E-14	-9.95E-14	-3.55E-14
-3.55E-14	-3.55E-14	1.03E-13

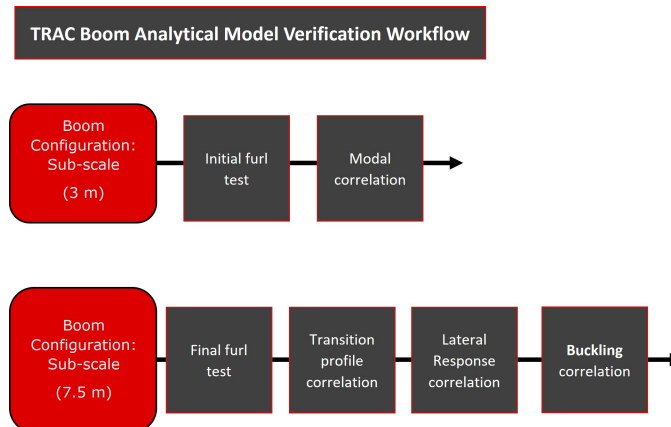
**Table 4 [D] Matrix (N-m)**

1.29E-01	4.25E-02	1.61E-03
4.25E-02	5.43E-02	1.61E-03
1.61E-03	1.61E-03	4.45E-02

With a laminate architecture designed to mitigate inner-flange buckling and shear stress failures in the bond region, eigenvalue buckling analyses followed. Having an initial viable buckling strength prediction allowed for higher fidelity finite element analyses (FEA) and a testing campaign to ensue.

## VI. FEM Verification Roadmap

The 30m TRAC boom has a high aspect ratio form factor and an open cross-section that allows for lateral-torsional displacement coupling. With a testing environment exacerbated by the overwhelming influence of gravity, it is



**Fig. 13 FEM Verification Workflow**

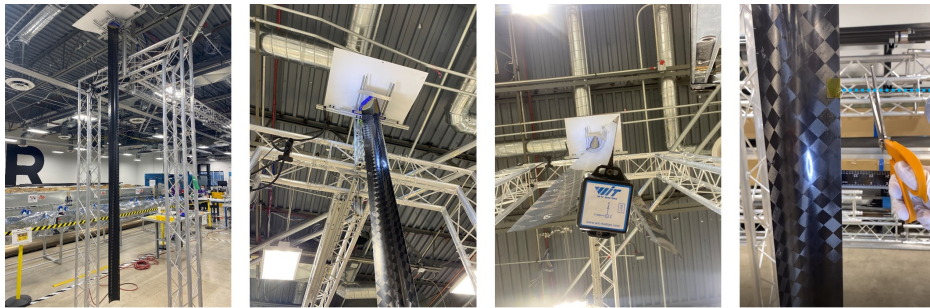


difficult to verify the buckling performance from 30m TRAC booms through ground testing alone. On the analysis side, finite element models in isolation are generally insufficient for qualifying structural margins when nonlinear behavior dominates. As such, a building block approach was adopted, using model-test correlation with progressively more-complex configurations, to ensure all factors that can contribute to such nonlinearities were identified and their compounding effects well-characterized. Figure 13 lays out this high-level approach in the verification workflow followed in developing the finite element model (FEM).

The general verification categories between test and analysis were divided between two TRAC boom test articles: a sub-scale 3 meter boom and a sub-scale 7.5 meter boom. All test articles had full-scale cross-sectional geometries; only the length dimension differed amongst the test booms. The testing and analysis campaign also coincided with the manufacturing development of the booms; the longer boom took more development time. The 3m and 7.5m booms were tested as they became available from the manufacturing team, and the analysis followed these enhanced testing capabilities appropriately.

### A. Sub-Scale 3 Meter Test Article

A 3m TRAC boom was produced and used to verify performance against inner-flange buckling via section V, following stowage and deployment off of a representative boom spool. With the success of this demonstration, confidence in the viability of the laminate construction improved, and consequently a 3m boom was mounted in a gravity offload fixture (in the vertical orientation to negate the effects of a 1 G environment) for modal testing, which is a low cost but effective check on the linear stiffness of the overall structure. (See Figure 14).



**Fig. 14 3m Boom Modal Test**

Global dimensions, overall mass and foundational stiffness of the backing structure were initial parameters that were adjusted in the FEM to match the test article. Additionally, natural frequencies were adjusted to account for air damping by the following relationship.

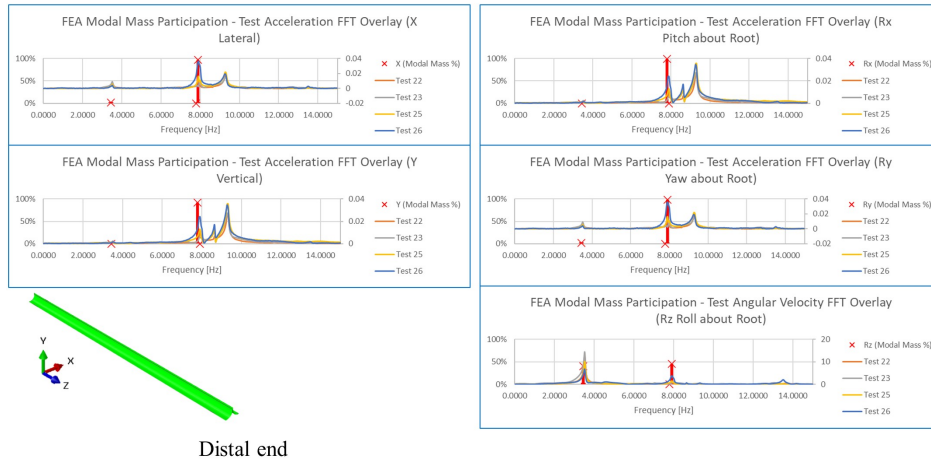
$$\frac{f_{air}}{f_{vacuum}} = \frac{1}{\sqrt{1 + \frac{M_{air}}{M}}}$$

The approach followed [11] where air mass was effectively coupled to the structure's different resonance modes, and natural frequencies were altered accordingly.  $f_{air}$  is the adjusted natural frequency in air,  $f_{vacuum}$  is the natural frequency in a vacuum (and in analysis),  $M_{air}$  is the virtual air-mass term that couples to the structure's mode shapes, and  $M$  is the mass of the boom.

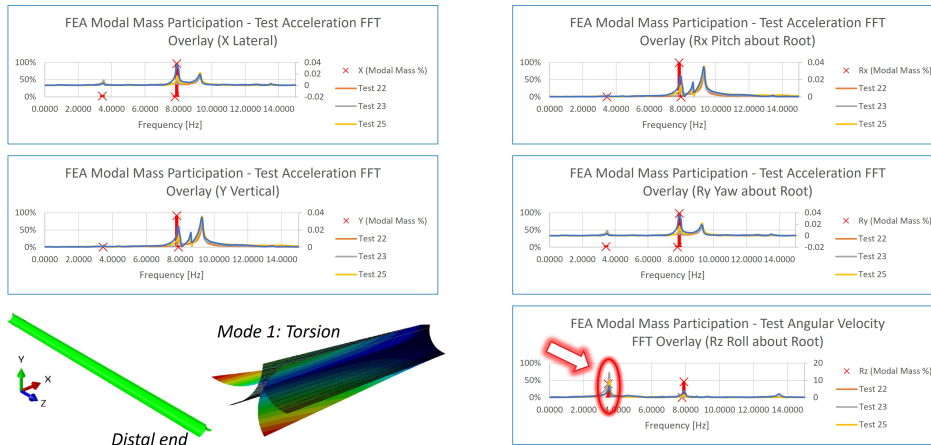
Next, a wireless tri-axial accelerometer was mounted to a 3D-printed wedge and adhered to the distal end of the boom. This instrumentation was also modeled in the FEM.

To perform the modal test, the distal end of the boom was preloaded through a tension wire. The wire was cut with shears, and time history response (linear accelerations and angular velocities) was captured and processed through a fast Fourier transform (FFT) algorithm. To correlate the FEM against this test data, modal mass participation was superimposed to the FFT data in respective orthogonal axes. In Figure 15, vertical red bars indicate natural frequency positions while curves depict directional responses along the frequency domain.

Simple mode shapes were characterized and correlated across test data and FEM predictions through interrogating response directional magnitudes at resonance frequencies. Figure 16 illustrates an example of this correlation exercise



**Fig. 15 Modal Mass-FFT Overlay**



**Fig. 16 Modal-Test Correlation for Torsion Mode**

for the torsional mode. The modal survey revealed relatively high values for modal effective moments of inertia in Rz (roll along Z-axis). Likewise, the FFT curve for angular velocity about the Z-axis showed resonance at the natural frequency for that mode. In the case of this torsional mode, the relevant natural frequency from analysis is -3% from the test data center frequency. Similar interrogation approaches applied in characterizing and correlating the other two critical modes shapes: a vertical mode and a lateral-torsional coupled mode.

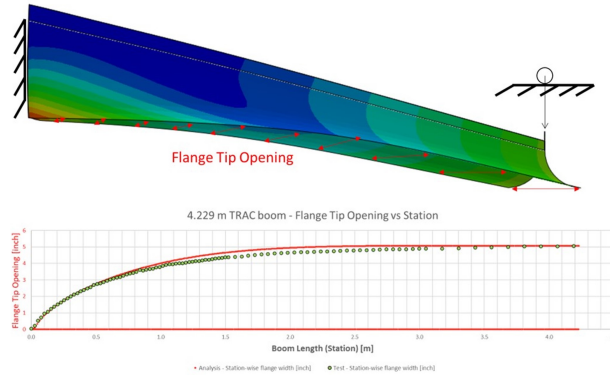
Overall, the FEM correlated very well with test data for the first two out of three modes. The highest error was -16% and was associated with the vertical mode. With these 3m boom tests, the laminate architecture's stowing stability and global stiffness and mass distribution were validated.

### B. Sub-Scale 7.5 Meter Test Article

Having built confidence into the initial FEM, the next step was to explore the complex nonlinear realm of TRAC boom structural mechanics. To further facilitate nonlinear response, we proceeded onto testing a higher aspect ratio 7.5m TRAC boom. After a final boom stowage and deployment cycle to verify stowage stability for a second attempt, the next simplest behavior to characterize was the transition profile from a flattened to fully-recovered cross-section.

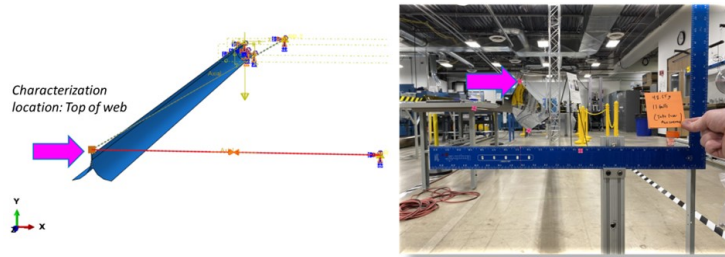
Here, the boom was clamped at the root end, while the flange tip-to-tip width was measured at fine increments from the flattened end to where the transition region terminated and the cross-section fully recovered. The same measurements

were then extracted from the FEM, and data was overlaid. This test checked the cross-sectional recovery rate of the boom from the spool tangency point to where it naturally regained its stress-free geometry. The nearly coincident model and test data points from Figure 17 built confidence in the analytical representation of the laminate stiffness and large deformation response.

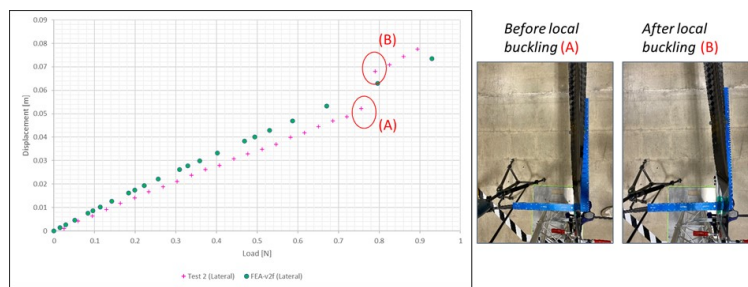


**Fig. 17 Transition Region Characterization**

With this successful correlation of the boom’s transition region length and shape, the lateral-torsional response mechanics were tested as shown in Figure 18. The boom was constrained at the root end and gravity-offloaded mid-span while load was introduced to a standoff tab at the distal web corner of the boom. In this manner, the coupled response under large displacements could be characterized and checked against analysis. Photogrammetry was utilized to characterize the displacements from the distal end under load.

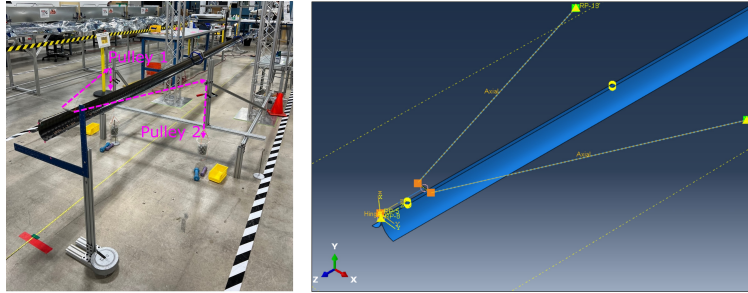


**Fig. 18 Lateral Load Test 1**



**Fig. 19 Lateral Load Test 2**

Load-deformation response from analytical predictions provided reasonable agreement with test results up until a point where the test data revealed a sudden increase in displacement that was not apparent in the analysis. By reviewing test evidence in Figure 19, a local buckle had occurred in the transition region near the root—an instability from a loading condition that is not flight representative. The largest displacement discrepancy between test and analysis was 17%, which was associated with the load at the onset of the local instability.

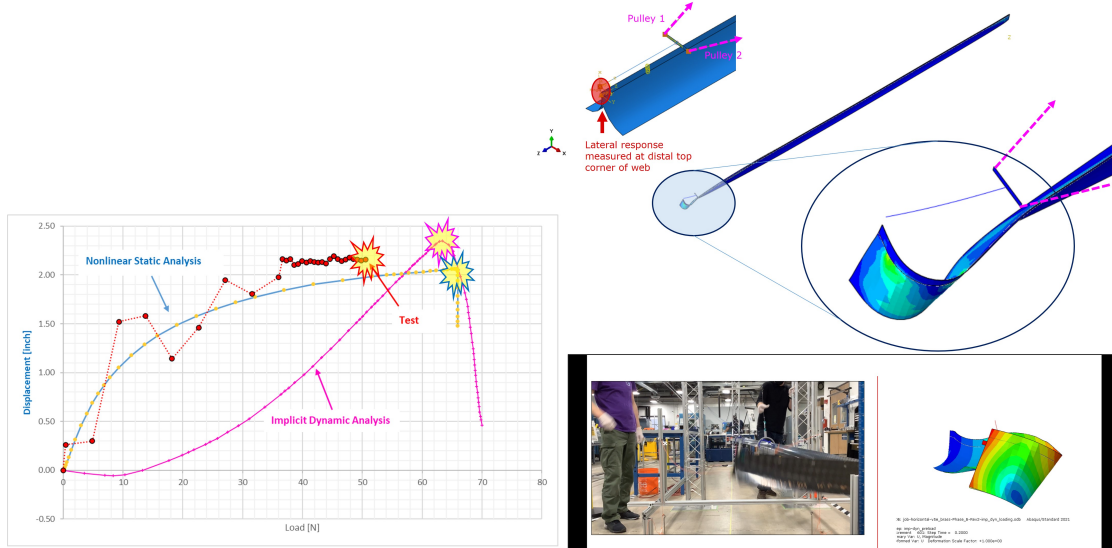


**Fig. 20 Combined Load Test 1**

The next step pursued capturing buckling behavior under axial loading of the 7.5m test article in a way that mimics the load condition of the 30m boom in flight. By this test, the boom design had matured to incorporate the distal end T-bar assembly—see section III.B.1 for full details. With this, the increased level of complexity attributed to capturing the loading condition from adjacent sail quadrants was addressed in Figure 20.

The objectives behind this step were to correlate the nonlinear tip response of the boom (under combined loading through the T-bar mechanism), to correlate the buckling load and to correlate the failure mode. The deformation metric was particularly challenging to define for meaningful response characterization between test and analysis, but ultimately the lateral displacement of the distal end web corner was selected due to the reliable history with photogrammetry as applied to that location. Two additional photogrammetry trackers were placed on the flange tips to track twist in addition to lateral displacement.

On the FEA front, the difficulty associated with obtaining a converged solution through Abaqus for this highly nonlinear simulation was approached through leveraging both the nonlinear static analysis and an implicit dynamic (quasi-static) analysis to explore the instability condition as well as the structural response as the loads approached the buckling condition. The left half of Figure 21 shows the overlay between the combined load-lateral deformation response from test and analyses, and the right half depicts the failure modes as witnessed during the test compared to analysis. The scattered results of the test were due to the boom responding to the load through bending and twisting rather than through pure lateral deflection. While it was proven to be difficult to obtain a converged solution to this simulation through a (nonlinear) static analysis (only 99% of the analysis step was able to converge), the implicit dynamic simulation was able to fully converge and is proven to be a powerful complement to, or replacement for, general static analyses. The test boom buckled at 50.5N of load from each pulley. The implicit dynamic analysis showed



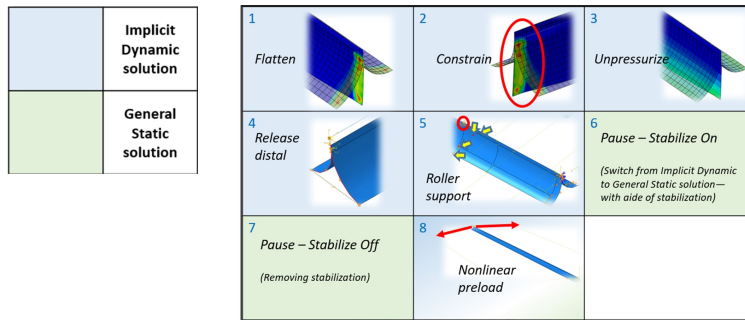
**Fig. 21 7.5m Boom Load-Deformation and Failure Mode Correlation**

buckling occurring at 63N from each pulley, and the nonlinear static analysis implied instability at around 67N each pulley. The tested buckling load was about 80% of the analytical prediction, which is consistent with knock-down effects observed in other cylindrical shells under compression loading due to geometric imperfections in the shells [10]. The bottom-right of Figure 21 illustrates the near identical match in collapse behavior at the distal end of the boom from the implicit dynamic simulation as it compared to the test failure mode. This failure condition as it manifested locally at the distal end steered the design update to incorporate a flange tip-to-tip bracing element as described in section III.B.2.

In summary, the 3m test article was purposed to perform a modal survey for key mode shapes, which were verified to correlate to the FEM though a superposition of response FFT data and modal effective mass. The 7.5m test article further tested nonlinear characteristics through studying flattening transition geometry and lateral response. The break-through milestone occurred at the buckling test when, under simulated flight axial loading, the FEM was able to predict all three key testing metrics: load-deformation response, buckling load and failure mode. It was with this success in model-test correlation that we believed we had a robust analytical model verification workflow and tools to develop and evolve testing and analytical model fidelity.

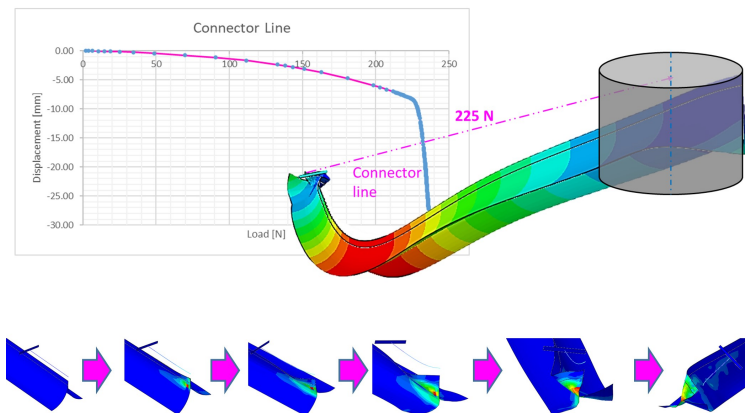
### VII. Initial 30m TRAC Boom Buckling Results

The most recent buckling simulations followed the Abaqus *Steps* workflow as shown in Figure 22.



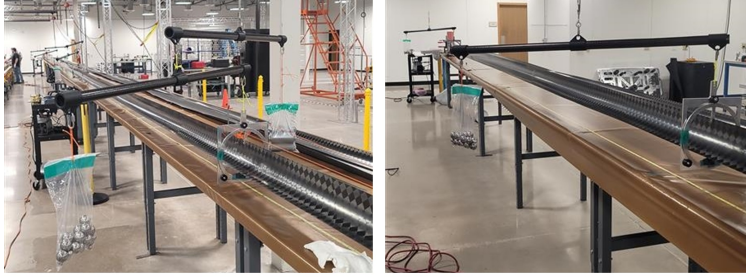
**Fig. 22 Abaqus Nonlinear Buckling Simulation Workflow**

Two nonlinear analysis types were utilized in Abaqus to explore global instability of the TRAC boom—the primary analysis type being implicit dynamic (quasi-static) analysis, with nonlinear general static analysis used to further support and/or bound the former predictions.



**Fig. 23 Baseline Buckling Load-Deformation Response**

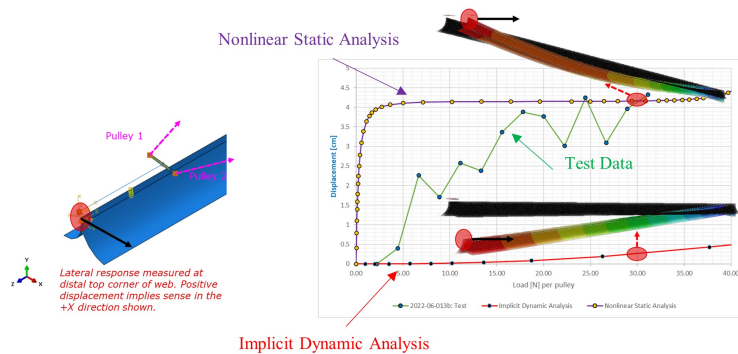
As shown in Figure 23, a load-deformation study of an artificial connector line between the distal web node to the hub centerline axis is leveraged to understand the overall TRAC boom response under flight compression loading and indications of the load at the onset of instability.



**Fig. 24 Whiffle Trees and DaVinci Assembly**

Concurrent with analytical simulations, a 30m TRAC boom was manufactured and tested but not without environmental challenges associated with testing under 1G. Gravity-offloading "Da Vinci" assemblies were utilized in combination with double-whiffle tree systems. See Figure 24. It is noted that this "gravity-offload" system does not compensate for gravity effects down the entire length of the boom but only at discrete offload points. However, careful considerations were made for the offload design to minimize the effects of gravity without over constraining the boom. Whiffle trees allow the freedom of lateral movement, while Da Vincis allow for two axis of rotation freedom. Near the fixed root, less lateral movement is expected, so single tier whiffle trees were used. The three whiffle trees closer to the distal end used double tier whiffle trees, which allow for much more vertical and lateral movement. When the booms were allowed to rotate freely, the effects of gravity had a run-away effect in the flanges where they sagged within the Da Vincis, causing more twist further down the boom. Furthermore, if the boom was allowed to twist 90 degrees during setup, the entire boom acted as a cantilevered spring, reacting to the off loading system in an uncontrolled manner.

During the loading procedure, the approach taken during the 7.5m test (as illustrated in Figure 20) was followed, and the resulting load-deformation overlay of the 30m test and analyses was produced in Figure 25. Two analysis types, implicit dynamic analysis and nonlinear static analysis, were utilized to simulate load-deformation response of the full-scale boom—and their results bound the test data.



**Fig. 25 Full-Scale Lateral Load-Displacement Response Analyses-Test Overlay**

At the current state of analysis in this report, the baseline buckling load is predicted at 225N with the analysis assuming simplified conditions, which include, but is not limited to, pristine, nominal geometries without the effects due to creep and thermal distortions. It is noteworthy that the TRAC boom buckling requirement, to maintain a factor of safety (FS) equal to or greater than 2 about a nominal operating 3N, has been demonstrated by test as being met. The 30m test article was loaded to an effective 58N (19x factor on the nominal operating load) *without* buckling. Barring model-test correlation at full-scale, the Solar Cruiser TRAC boom appears to be well over-designed. However, in order to build confidence in the analytical buckling predictions, better full-scale testing and an assessment of geometric imperfections will be needed to determine the actual load capacity of the design.

## VIII. Conclusion

The NASA Solar Cruiser relies on a challenging form of propulsive technology. In order to enable novel orbits and far-reaching destinations, the overall system must be gossamer, expansive in dimensions and lightweight as possible, to allow for adequate characteristic accelerations. The spacecraft depends on utilizing high aspect ratio booms that are stiff and stable enough to support sail tensions without buckling. TRAC booms have the highest bending stiffness for a given flattened height of any rollable structural booms but not without cost. The open cross-section not only yields low torsional stiffness but also produces problematic bending-torsion coupling, both of which can translate to poor dimensional stability (affecting spacecraft attitude determination and control) and buckling performance. The problem becomes ever more pressing when one realizes how inaccurate traditional linear finite element simulations, i.e. eigenvalue buckling simulations, are when characterizing TRAC booms under load. Adding to this complication, a full scale 30 meter TRAC boom, let alone the overall system, cannot be tested and validated under the influence of Earth's gravity, as adequate gravity off-loading solutions at this scale are nonexistent. The behavior of the TRAC boom is not intuitive—and neither is the high performance that these structures are demonstrating in testing against buckling.

With the unintuitive and nonlinear nature of these designs and the highly positive performance that they are demonstrating in testing against buckling, one realizes that in order to harness the capability of these booms for very large deployable aperture architectures, such as solar sails, an incremental, building block approach to model-test correlation needs to be adapted in order to build confidence into the finite element models. Through initial testing to validate linear, small-displacement modal response predictions, to more developed, rigorous testing to exercise large-displacement nonlinearities and trigger instabilities with higher-aspect ratio booms, the characteristics of the TRAC boom are beginning to become understood, as is the analytical strategies employed to study apparent behaviors.

The current TRAC boom design is proven to meet the buckling requirement purely through test. The fidelity of FEM has been vetted by test correlation. FEA predicts factors of safety greater than the requirement ( $FS = 2$ ). Additional structural testing (including to failure) and FEM updating will continue to add critical insight in bridging the gap between possible hardware performance in flight to FEA predictions by virtue of developing greater confidence in our understanding of highly nonlinear structural responses under interaction with the system level assembly and mechanisms. At this point, we are confident that the TRAC boom architecture is the solution to improving greater sail tension loads while inhibiting detrimental failure modes.

Additional analyses to account for sensitivity studies on geometric imperfections, laminate properties, and others would continue to add value in broadening the predicted range in buckling knock-down factors and expected failure modes to the baseline analysis. Nonetheless, engineering judgment deems that the current TRAC boom design is successful in meeting the boom buckling requirement through a collection of FE simulations and a comprehensive testing campaign.

## Acknowledgments

The work herein was funded by NASA under Marshall Spaceflight Center contract 80MSFC21CA008. The authors would like to acknowledge and express their gratitude to the NASA Langley Research Center for their guidance and support through numerous technical interchanges. The inputs from Dr. Jay Warren and Dr. Olive Stohlman have proved invaluable in representing solar sail global mechanics and resolving FEA challenges. The support from Dr. Marc Schultz, Dr. Cyrus Kosztowny and Lauren Simmons on laminate properties testing and providing insight and independent structural analyses is much appreciated.

## References

- [1] Murphey, T. W. and Banik, J., "Triangular rollable and collapsible boom". US Patent No. 7,895,795, March 1, 2011.
- [2] Banik, J. and Murphey, T., "Performance Validation of the Triangular Rollable and Collapsible Mast," in Proceedings from the 24th Annual AIAA USU Conference on Small Satellites, Logan, UT, 2010.
- [3] Murphey, T. W., Turse, D., and Adams, L., "TRAC Boom Structural Mechanics," in *4th AIAA Spacecraft Structures Conference*, Grapevine, TX, 2017.
- [4] Cox, K., and Medina, K., "Scalability of Triangular Rollable and Collapsible Booms", in *AIAA SciTech Forum*, San Diego, CA, 2019.
- [5] Johnson, Les Curran, Frank Dissly, Richard Heaton, Andrew Turse, Dana. (2020). The Solar Cruiser Mission -Demonstrating Large Solar Sails for Deep Space Missions.

- [6] Cox, K., and Medina, K., "An Investigation of Inner Flange Buckling in Furlable Composite Booms," in *Proceedings of the American Society for Composites—Thirty-third Technical Conference*, Seattle, 2018.
- [7] Leclerc, C., Pedivellano A., and Pellegrino, S., "Stress Concentration and Material Failure during Coiling of Ultra-Thin TRAC Booms," in *AIAA Spacecraft Structures Conference*, Kissimmee, FL, 2018.
- [8] Leclerc, C. and Pellegrino, S., "Reducing Stress Concentration in the Transition Region of Coilable Ultra-Thin-Shell Booms", in *AIAA SciTech Forum*, San Diego, CA, 2019.
- [9] Leclerc, C., and Pellegrino, S., "Characterization of Ultra-Thin Composite Triangular Rollable and Collapsible Booms", in *4th AIAA Spacecraft Structures Conference*, Grapevine, TX, 2017.
- [10] "Buckling of Thin-Walled Cylinders," NASA SP-8007, September 1965.
- [11] Blevins, R. D., *Formulas for Dynamics, Acoustics and Vibration*, Wiley, 2015.